Limnol. Oceanogr., 36(2), 1991, 362–369

Feeding currents and energy dissipation by *Euchaeta rimana*, a subtropical pelagic copepod

Abstract—Based on the pathlines of the flow field of the pelagic copepod *Euchaeta rimana*, we calculated some characteristics of the velocity gradient field: vorticity, shear, and squared rates of strain. We found that this copepod created a sheared laminar flow field, which is most intense near the moving paired second antennae and transports a volume of water similar to that measured in feeding experiments. The far-field flow is a combination of first-order and higher order scanning currents that serve to overcome nega-

Acknowledgments

We thank Ken Denman, Mimi Koehl, and Celia Marrasé for their interest and encouragement in our study. We also thank an anonymous reviewer for substantial help.

J.Y. acknowledges support by the Office of Naval Research (grant N00014-87-K-0181). B.S. acknowledges support by the Natural Sciences and Engineering Research Council of Canada (grant OGP0000822). J.R.S. acknowledges support by the National Science Foundation (grants OCE 84-16261 and OCE 87-19984).

Contribution 778 from the Marine Sciences Research Center, State University of New York at Stony Brook.

tive buoyancy, enhance prey detection and capture, and limit detectability by predators. In the feeding current, the flow intensity is comparable to that of small-scale turbulence while the length scale is one order of magnitude smaller than that of shear-containing turbulent eddies. Viscous energy dissipation rates within the feeding current are higher than those due to turbulence. However, spatially averaged energy dissipation by feeding currents is less than that of turbulence with the possible exception of within a very dense swarm of copepods. Spatially averaged vertical eddy diffusivities caused by feeding currents are several orders of magnitude smaller than that caused by turbulence in the surface mixed layer.

Velocity structure and energy transfer in the ocean occur at multiple scales. Here, we present a study at the scale of milliseconds and millimeters. We evaluate the contribution of hydrodynamic disturbances (henceforth called feeding currents for convenience) generated by zooplankton to small-scale turbulence in the sea. We also examine how the structural properties of these feeding currents are related to prey detection, positional stability, and predator avoidance.

With a laser-illuminated, video-monitoring system (Strickler 1985), it is possible to follow the movements of freely swimming copepods as well as the paths of particles as small as 10 μm disturbed by a 1–10-mm zooplankter. In this study, we have examined the behavior of the pelagic predatory copepod *Euchaeta rimana.*

Euchaeta rimana is a subtropical, surface-dwelling, open-ocean copepod common in the plankton of the North Pacific central gyre where it is one of the larger members of the copepod community (prosome length of the adult female, ~25 mm: Hayward 1980; McGowan and Walker 1979). These copepods were collected with a 333-μm-mesh, 1-m-diameter net towed from 100 m to the surface 2 km outside Kaneohe Bay, Hawaii, where depths are >200 m and open-ocean copepods can be obtained. Live animals collected in the hauls were sorted carefully into seawater and kept at 20°C. The culture vessels were supplemented with a variety of small copepods (~500-μm prosome length) for food. These small copepods were collected with a 110-μm-mesh, 0.5-m-diameter net towed in Kaneohe Bay near Coconut Island. Under these conditions, *E. rimana* has been easily kept in the laboratory for 1 month or longer.

Within the first 2 weeks after collection, observations of the swimming behavior of the copepods were recorded by J. Yen at J. R. Strickler's laboratory, then at the University of Southern California. Prey and predatory copepods were transported from Hawaii to Los Angeles in thermally insulated containers. Animals arrived in excellent condition.

The basic system of laser photography is a modification of the Schlieren optical pathway (*see* Strickler 1985) in which an object forms a light image on a dark background. The light energy of 0.1 μW cm^{-2} had no observed effect on the swimming behavior of *E. rimana*; when exposed to the laser light, the copepod did not change its behavior from that in dim light. The speed of the videotapes was 30 frames s^{-1}. The activity of the copepods was recorded in the dark in a tank of the following dimensions: 12 × 12 × 15 cm (length × width × height). The tank was filled with 1 liter of glass-fiber-filtered seawater. Ten to 20 *E. rimana* were placed in the tank with 20–40 small copepods added as prey. Prey were either from Kaneohe Bay or from off Long Beach, California. To make sure that the behavior was generally representative, we made observations of several different individual copepods on different days. These copepods were selected from different net hauls taken five separate times between August 1986 through February 1987.

With frame-by-frame analyses of the videotapes, the drawing of the flow field relative to a stationary animal was constructed by tracing the paths taken by algal particles (*Dunaliella tertiolecta*) entrained in the flow. The copepod in this scene is sufficiently far from the walls of the container so that no wall effect can be discerned in the streamlines of the flow field. Flow velocities decreased away from the copepod to velocities matching background motion. This decrease occurred well away from the walls of the container. As found by Strickler (1985), the flow field of copepods consists of steady, sheared, laminar flow (Fig. 1).

To examine kinematic characteristics of

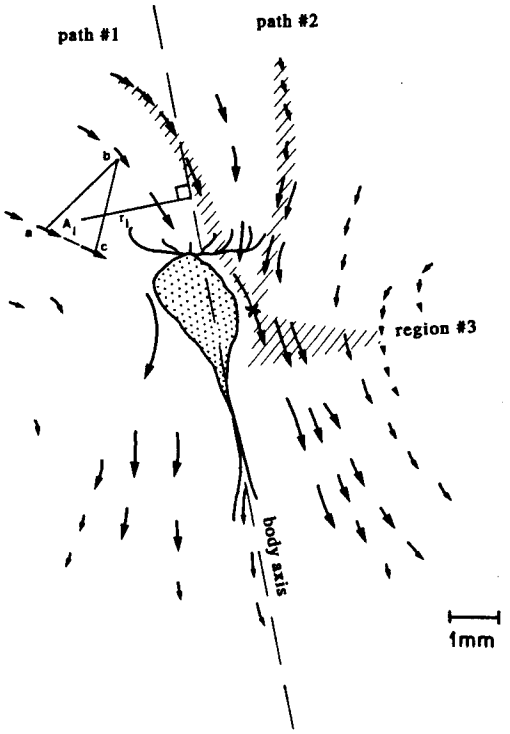

Fig. 1. Flow field of *Euchaeta* feeding current on the dorsal-ventral plane nearly perpendicular to the stretched first antennae and also parallel to the body axis. The camera was focused on the body and only algal particles in sharp focus were followed; i.e. they were moving within the focal plane during the observation period. Arrows indicate pathlines of 10–20-μm algal particles in the time interval of 0.3 s. The arrow vector divided by 0.3 s represents the particle velocity vector at the midpoint of the arrow. Particles very close to the animal cannot be resolved because of the shadow effect (Strickler 1985). Velocities are taken as zero at the body surface of the copepod. The animal's body axis is marked with a dashed line. Groups of 3-point velocity estimates at positions marked *a, b, c* are used to calculate velocity gradients and strain rates of the ith triangle of area A_i whose apices are at *a, b, c*. The perpendicular distance of the centroid of A_i from the animals body axis is r_i.

feeding current fields, we define a coordinate system (x, y) so that the x-axis is perpendicular to the animal's body axis and the y-axis is along the body axis and positive upward. Each arrow in Fig. 1 therefore defines the velocity vector of a particle at the midpoint of the arrow. The particle velocity is decomposed into components u and v along x and y respectively. To compute velocity gradients, we consider three neighboring velocity vectors, such as those labeled *a, b, c* in Fig. 1. The velocity gradients (shear, stretching deformation, divergence, and vorticity) at the centroid of this triangle were calculated from the velocity vectors *a, b, c,* and their positions with the method of Okubo and Ebbesmeyer (1976). A total of 118 triangles are considered so as to completely fill the space surrounding *E. rimana* out to the limit of the area where velocity measurements were made.

In general, a high velocity of $\sim$0.5 cm s^{-1} is observed in the vicinity of the animal and a typical velocity of the feeding current is a few mm s^{-1}. For *E. rimana,* the Reynolds number estimated for the second antennae is 2. In general, Reynolds numbers associated with copepod feeding appendages range from 0.02 to 5 (Koehl and Strickler 1981; Andrews 1983).

There are regions of strong vorticity (Fig. 2) and shear (Fig. 3) closest to the moving second antennae and extending around the body of *Euchaeta.* The vorticity field is characterized by regions of alternating rotation, where rotations of the opposite sense are on either side of the copepod. In front of the first antennae, the feeding current possesses a relatively strong shear and stretching rate. Although this feature of the velocity gradient field is obtained with *Euchaeta,* it is expected to be common among many species of swimming and feeding zooplankton. Thus, for a herbivorous copepod, the convergent feeding current produces a shear and stretching rate field in front of the animal so that a chemical exudate cloud around an entrained alga may be elongated in the streamwise direction by stretching and the shear-diffusion effect. Our calculations of the velocity gradient field support the general functional form of the theoretical flow pattern of feeding current assumed by Andrews (1983) in order to model chemosensory perception of algae by copepods. Some of the flow-field parameters used by Andrews (1983) are different, however, from ours.

Andrews used a velocity with a vertical e-folding scale of 1.8 mm and a horizontal e-folding scale of 0.2 mm. To find an approximate vertical e-folding scale from our data, consider the hatched paths 1 and 2 in

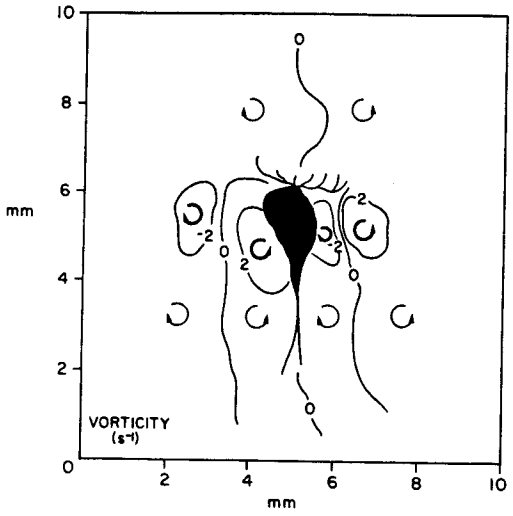

Fig. 2. Vorticity field, $(\partial V/\partial x) - (\partial U/\partial y)$, calculated on the basis of Fig. 1. Clockwise arrows indicate negative vorticity and anticlockwise arrows indicate positive vorticity.

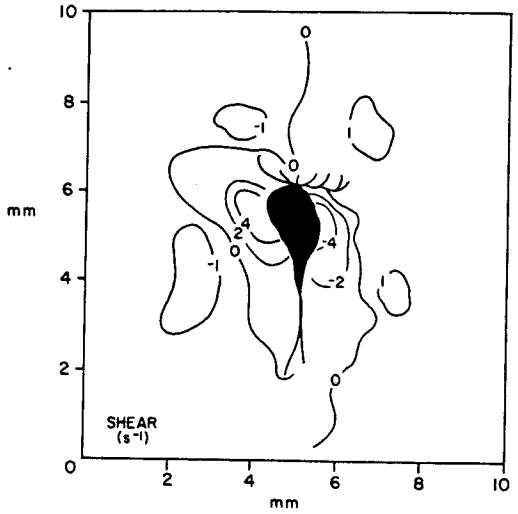

Fig. 3. Shearing rate field, $(\partial U/\partial y) + (\partial V/\partial x)$, calculated on the basis of Fig. 1.

Fig. 1 as trajectories that intersect approximately at the point marked ×. We then consider how current speed varies with distance r from this point, for the two paths. In both cases we find an exponential dependence with an e-folding scale in the range of 2.4–2.8 mm (Fig. 4A). Similarly, the velocity transverse to region 3 in Fig. 1 varies exponentially with radial distance from the body axis (Fig. 4B). In this case we find a horizontal e-folding scale of 1.8 mm. The ratio of vertical e-folding scale to horizontal e-folding scales is about 1.4 for our observational data, whereas the value corresponding to Andrews' choice of parameters was 9.

Childress et al. (1987) undertook a theoretical study of the scanning currents that organisms use to locate food. They classified several theoretical scanning mechanisms in the following way. First-order scanning mechanisms have radial and nonradial components of velocity that drop off inversely with distance from the current generating point. Higher (nth order where n = 2, 3, . . .) order mechanisms have a radial component of velocity that drops off as distance raised to the power $-n$. Nonradial velocity components drop off, however, as distance to a power of -2 for all higher order scanning mechanisms. For a predator that maintains its position against negative buoyancy we expect that first-order scanning, which develops thrust, will be required. One side effect of first-order scanning is that the velocity field drops off only slowly with distance, and therefore is relatively easily detected by predators. If we consider velocity at points that are far away from × in Fig. 1, we find that an inverse power law will reasonably describe the decay of the radial velocity with radial distance from × (Fig. 4C). In region 3 of Fig. 1, however, we find that even far from the body axis the decay of transverse velocity (transverse to the orientation of region 3) with radial distance from the body axis does not fit an inverse-power law.

Along path 1, the far-field current speed is largest, but it decays as radial distance raised to a power of -1.5. This pattern suggests a mix of first- and higher order scanning mechanisms. Along path 2, where current speeds are smaller, the decay is as radial distance raised to a power of -1.0, which indicates a first-order scanning mechanism. It appears that *Euchaeta* uses a mix of scanning mechanisms in such a way that those parts of its feeding current that are more intense fall off more rapidly with distance from the organism. In this manner it overcomes its negative buoyancy, generates a

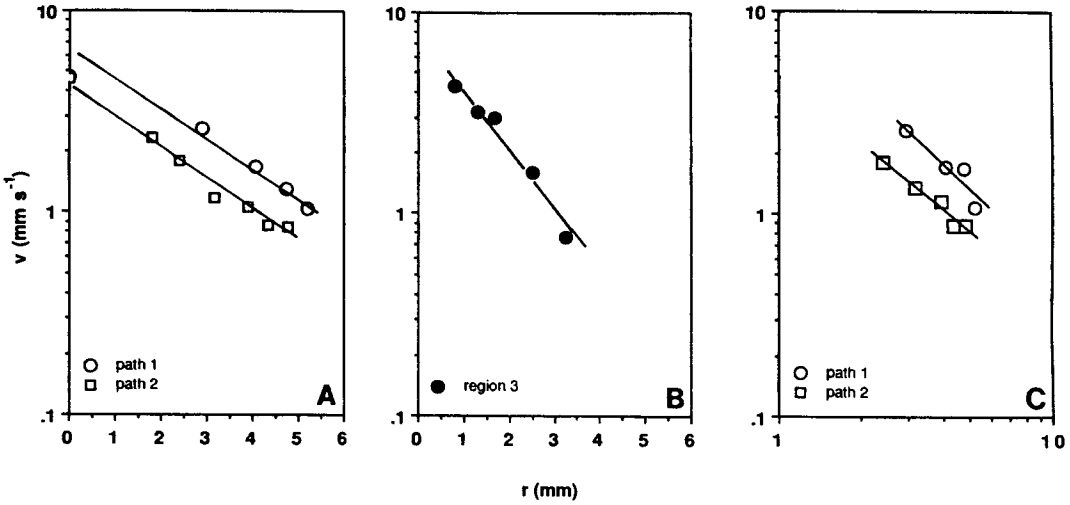

Fig. 4. A. The log of velocity vs. distance from × (in Fig. 1) along paths 1 (○) and 2 (□). Velocity is proportional to $e^{-\beta r}$, where β = 2.2/5.3 or 0.42 and 2.15/6.1 or 0.35 for paths 1 and 2. The e-folding scale for path 1 is 2.4 mm and 2.8 mm for path 2. B. The log of speed vs. radial distance from the animal's body axis in region 3. Here, β = 0.82 and the e-folding scale is 1.2 mm. C. The log velocity vs. log of radial distance from × for points >2 mm from ×, along paths 1 (○) and 2 (□). Here, velocity is proportional to $r^{-\gamma}$, where γ = 1.5 and 1.04 for paths 1 and 2.

feeding current, and restricts the far-field current signals that would advertise its position to predators.

The water is brought to the animal in front of its antennae, perpendicular to the plane of the first antennae but parallel to the plane of the setae on the antennae. These setae, aligned in the flow, are important mechanosensors for the copepods (Gill 1986; Yen and Nicoll 1990) and thus are well positioned for detecting deformations in the streamlines. If we assume axisymmetric inflow, water is brought toward the copepod at a rate of 1 mm in 0.3 s or 0.3 cm s^{-1}, through an area of about $\pi(0.2\text{ cm})^2 = 0.13$ cm^2. This calculation gives a volume filtered of 0.038 $cm^3\ s^{-1}$ or 3.3 liter d^{-1}. It approximates clearance rates measured for this predatory copepod which can consume 65 prey d^{-1} at 25 prey $liter^{-1}$ (Finn 1983).

We imagine that the strong counteracting vorticity field in the mouthpart regions of *Euchaeta* (Fig. 2) can serve to stabilize the body axis while the animal is generating its feeding current. This self-controlling fluid mechanical effect has not been discussed by previous investigators. The flow field is created mainly by the beating of the second antennae of the copepod. The second antenna is biramous, with one branch behind the animal (dorsal side) and the other in front of it (ventral side), both beating at the same frequency. In this case, the copepod beats its antennae at just the rate needed to keep it hovering, stationary in the water, moving neither forward, backwards nor up, down. A balance is struck in the forces of gravity and flow velocity. In this sequence of behavior, this otherwise cruising predator may silently "sit-and-wait" for a prey to be drawn into its flow field (Gerritsen and Strickler 1977).

In the vicinity of the animal, the speed changes by ~0.4 cm s^{-1} in 0.2 cm giving a shear of 2 s^{-1}. The shear is of order 1 s^{-1} for the feeding current as a whole. By inspection of Fig. 1, we find that cross-stream and along-stream dimensions of the feeding current are 0.5 and 1.0 cm, respectively. Beyond these distances, the currents are greatly reduced from their values near the animal.

At scales l_0 = 12 and 7 cm, the results of Denman and Gargett (1988) indicate a peak in the spectrum of turbulent shear for viscous energy dissipation rates $\epsilon = 10^{-4}$ and $10^{-3.3}$ $cm^2\ s^{-3}$, respectively. This peak in the shear spectrum occurs at scales l_0 that

are 37 times as great as the Kolmogorov length scale $\eta = (\nu^3/\epsilon)^{1/4}$ for both the values of ϵ above. Looking at the shear spectrum of Denman and Gargett, we see that effectively all the shear is removed at scales $l_s = 2\pi\eta$. We define a time scale for the peak shear eddies to be $\tau_0 = (7.5\nu/2\epsilon)^{1/2}$, which in the case of their results gives $\tau_0 = 2\tau$ where $\tau = (\nu/\epsilon)^{1/2}$ is the Kolmogorov time scale. Similarly we find a relative velocity scale v_0 over a separation distance l_0 to be $v_0 = 20v$, where $v = (\epsilon\nu)^{1/4}$ is the Kolmogorov velocity scale.

Oceanic energy dissipation rates in the upper mixed layer are typically in the range $\epsilon = 10^{-2}$–10^{-4} cm^2 s^{-3} (*see* figure 4 of Faller 1971). This rate results in turbulent eddies that have their peak in the shear spectrum at scales $l_0 = 4$–12 cm and effectively no shear at scales $< l_s = 0.6$–2 cm. Clearly the copepod eddies have length scales that are about an order of magnitude $< l_0$ and similar to or $< l_s$. The peak shear in the turbulence will be between $\tau_0^{-1} = 0.05$ and 0.5 s^{-1} for $\epsilon = 10^{-2}$–10^{-4} cm^2 s^{-3} respectively. Except in the most energetic turbulence, copepod eddies have shears that are generally an order of magnitude higher than that of the oceanic turbulence. Turbulent velocities in these peak shear-containing eddies are $v_0 = 0.6$–1.9 cm s^{-1} for $\epsilon = 10^{-2}$–10^{-4} cm^2 s^{-3}. The intensity of these turbulent eddies is, therefore, similar to the intensity of copepod eddies.

Consider that the energy cascade is caused by the Reynolds stresses due to vortex stretching. Thus the transfer of energy to smaller scales is caused by the large-scale shears stretching small eddies (Tennekes and Lumley 1972). The addition of energy at some scale will cause an increased amount of eddy energy transfer at scales smaller than that scale, but not at scales greater than that scale. We thus conclude that copepods would not affect the cascade of turbulent energy to dissipation scales. *Euchaeta* eddies in a dense swarm, however, may dominate oceanic turbulence at scales similar to or $< l_s = 0.6$–2 cm for $\epsilon = 10^{-2}$–10^{-4} cm^2 s^{-3}. Further the feeding currents have scales that are sufficiently large to make them measurable with either heated-film or airfoil probes.

The feeding-current eddies have vertical length and velocity scales of 1 cm and 0.5 cm^{-1}. Considering a volume of 1 cm^3 that contains such an eddy, we could ascribe a local diffusivity $D \sim 1$ cm $\times$ 0.5 cm s^{-1} = 0.5 cm^2 s^{-1}. Average diffusivity in a larger volume that is not completely filled with eddies, however, will be given by

$$\bar{D} = Dn \times 10^{-6}$$

where n is the number of *Euchaeta* in 1 m^3 of seawater. In a dense swarm ($n = 1{,}000$), $\bar{D} = 0.5 \times 10^{-3}$ cm^2 s^{-1}, which is much larger than the molecular diffusivity ($\sim 10^{-5}$ cm^2 s^{-1}) but considerably smaller than the vertical eddy diffusivity in the interior ocean (Munk 1966). The above value for $\bar{D}$ is very much less than the value of 5 cm^2 s^{-1} in the surface mixed layer that can be obtained from the results of Denman and Gargett (1988). On the other hand $\bar{D} = 0.5 \times 10^{-3}$ cm^2 s^{-1} is quite consistent with Munk's (1966) estimate of 10^{-3} cm^2 s^{-1} for the upper limit of diffusivity associated with biological mixing.

The high shears observed in the feeding current indicate that it might be valuable to calculate the rate at which viscosity dissipates energy in the feeding current. For this calculation, it is convenient to consider a cylindrical polar coordinate system where z is oriented along the body axis, r is the radial distance from the body axis, and θ is an azimuthal angle. The velocity components are U_z, U_r, U_θ along the z, r, θ directions. Assuming axisymmetry of the feeding current (as depicted in figure 8 of Strickler 1985), we can calculate the viscous energy dissipation per *Euchaeta* eddy, Φ, as

$$\Phi = 2\pi\rho\nu \sum_{i=1}^{N} r_i A_i \cdot \left[\left(\frac{\partial U_z}{\partial z}\right)_i^2 + \frac{1}{2}\left(\frac{\partial U_r}{\partial z} + \frac{\partial U_z}{\partial r}\right)_i^2 + \left(\frac{\partial U_r}{\partial r}\right)_i^2 + \left(\frac{U_r}{r}\right)_i^2\right] = 9.3 \times 10^{-10} \text{ W individual}^{-1}. \quad (1)$$

In this equation ρ is the density of water, $\nu = 10^{-2}$ cm^2 s^{-1} the kinematic viscosity at 20°C, A_i the area of the ith triangle formed

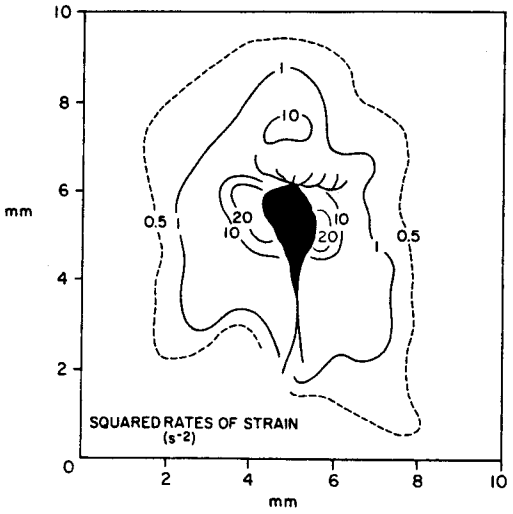

Fig. 5. Field of the total squared rates of strain calculated on the basis of Fig. 1. This field is used to estimate the energy dissipation rate by viscosity (*see Eq. 1*).

with three velocity vectors at its vertices (Fig. 1), r_i the radial distance from the body axis to the centroid of the ith triangle, and the bracketed term on the right-hand side the squared rate of strain (Fig. 5) computed from the velocity components at the corners of the ith triangle (Okubo and Ebbesmeyer 1976).

The assumption of axisymmetry means that we have ignored strains due to gradients in U_θ and any dependence of U_x and U_r on θ. We are forced to make this assumption due to the two-dimensional nature of our data. To test this assumption, we note that axisymmetry and incompressibility (i.e. the three-dimensional flow is nondivergent) require

$$\nabla \times \mathbf{U} = \frac{\partial U_x}{\partial z} + \frac{\partial U_r}{\partial r} + \frac{U_r}{r} = 0.$$

Computing $\nabla \times \mathbf{U}$ from the data gave values that were typically only a third as large as the shear. Hence the assumption of axisymmetry is reasonable to a first-order approximation and might be expected to cause our calculations of Φ to be underestimated by only $\sim 10\%$ [$\sim(1/3)^2$].

The space in which velocity observations were made surrounding the animal had a total volume

$$V = 2\pi \sum_{i=1}^{N} r_i A_i$$

of 0.34 cm^3. The velocity field has not diminished to zero outside this volume, but from Fig. 5, it is plain that the strain field is substantially reduced at the outer limits of the volume measured. We expect that extending the area in which velocity measurements are made would not greatly modify our calculation of the amount of energy dissipated.

Dividing Φ by ρ and the volume (V) of the strain field gives 2.8×10^{-2} cm^2 s^{-3} for the average dissipation rate inside the volume of the feeding current. This value is beyond the upper end of the typical oceanic (bulk) dissipation rates in the surface mixed layer and is consistent with results obtained from our earlier scaling arguments. The locally elevated energy dissipation rate by marine organisms may not be surprising, however. During simultaneous acoustic and microstructure measurements from a submarine, Farmer et al. (1987) observed a sudden increase by a factor of 100 in energy dissipation rate that coincided with the submarine's passage through water vacated by a school of fish.

If we denote the number of *Euchaeta* in 1 m^3 of seawater by n, the average energy dissipation rate due to the population is calculated by

$$\epsilon = 0.93 \times 10^{-8} n \text{ cm}^2 \text{ s}^{-3}. \qquad (2)$$

For n = 1, 10, 100, and 1,000, ϵ is given by 1×10^{-8}, 1×10^{-7}, 1×10^{-6}, and 1×10^{-5} cm^2 s^{-3}. The average values are generally smaller than those of oceanic turbulence in the upper mixed layer. In a dense patch of *Euchaeta*, however, the average energy dissipation rate would be about the same order of magnitude as oceanic turbulence in the thermocline.

In conclusion, our study, though still preliminary, suggests several interesting results. Physical mixing and energy dissipation are generally much greater than that due to copepod eddies. Copepod eddies have

a smaller length scale and much larger shear, however, than do shear-containing turbulent eddies in the ocean. Thus, in the vicinity (within 1 cm) of copepod eddies, we expect that biological activity will provide a greater contribution to velocity shear, viscous energy dissipation, and rates of change of tracer microstructures. Under special circumstances (passage of a school of fish or dense swarms of copepods in the thermocline), viscous energy dissipation may be mainly due to biological energy sources rather than physical turbulence.

Jeannette Yen

Marine Sciences Research Center
State University of New York
Stony Brook 11794-5000

Brian Sanderson

Department of Physics, and
the Ocean Science Centre
Memorial University of Newfoundland
St. John's A1B 3X7

J. Rudi Strickler

Center for Great Lakes Studies
University of Wisconsin–Milwaukee
600 East Greenfield Ave.
Milwaukee 53204

Akira Okubo

Marine Sciences Research Center
State University of New York
and
Ecosystems Research Center
Cornell University
Ithaca, New York 14853-2701

References

ANDREWS, J. C. 1983. Deformation of the active space in the low Reynolds number feeding currents of calanoid copepods. Can. J. Fish. Aquat. Sci. **40:** 1293–1302.

CHILDRESS, S., M. A. R. KOEHL, AND M. MIKSIS. 1987. Scanning currents in Stokes flow and the efficient feeding of small organisms. J. Fluid Mech. **177:** 407–436.

DENMAN, K. L., AND A. E. GARGETT. 1988. Multiple thermoclines are barriers to vertical exchange in the subarctic Pacific during SUPER, May 1984. J. Mar. Res. **46:** 77–103.

FALLER, A. J. 1971. Oceanic turbulence and the Langmuir circulations. Annu. Rev. Ecol. Syst. **2:** 201–236.

FARMER, D. D., G. B. CRAWFORD, AND T. R. OSBORN. 1987. Temperature and velocity microstructure caused by swimming fish. Limnol. Oceanogr. **32:** 978–983.

FINN, J. A., JR. 1983. Reproduction and feeding in the tropical, carnivorous copepod *Euchaeta rimana* Bradford. M.S. thesis, Univ. Hawaii. 55 p.

GERRITSEN, J., AND J. R. STRICKLER. 1977. Encounter probabilities and community structure in zooplankton: A mathematical model. J. Fish. Res. Bd. Can. **34:** 73–82.

GILL, C. W. 1986. Suspected mechano- and chemosensory structures of *Temora longicornis* (Copepoda: Calanoida). Mar. Biol. **93:** 449–457.

HAYWARD, T. L. 1980. Spatial and temporal feeding patterns of copepods from the North Pacific Central Gyre. Mar. Biol. **58:** 295–309.

KOEHL, M. A. R., AND J. R. STRICKLER. 1981. Copepod feeding currents: Food capture at low Reynolds number. Limnol. Oceanogr. **26:** 1062–1073.

MCGOWAN, J. A., AND P. W. WALKER. 1979. Structure in the copepod community of the North Pacific Central Gyre. Ecol. Monogr. **49:** 195–226.

MUNK, W. H. 1966. Abyssal recipes. Deep-Sea Res. **13:** 707–730.

OKUBO, A., AND C. C. EBBESMEYER. 1976. Determination of vorticity, divergence, and deformation rates from analysis of drogue observations. Deep-Sea Res. **23:** 349–352.

STRICKLER, J. R. 1985. Feeding currents in calanoid copepods: Two new hypotheses, p. 459–485. *In* M. S. Laverack [ed.], Physiological adaptations of marine animals. Soc. Exp. Biol.

TENNEKES, H., AND J. L. LUMLEY. 1972. A first course in turbulence. Mass. Inst. Technol.

YEN, J., AND N. T. NICOLL. 1990. Setal array on the first antennae of a carnivorous marine copepod, *Euchaeta norvegica*. J. Crust. Biol. **10:** 218–224.

Submitted: 17 July 1989
Accepted: 25 October 1990
Revised: 28 November 1990

Erratum

The first sentence of the third paragraph of the note by Jeannette Yen et al. (March 1991: Vol. 36, No. 2, p. 363) should read: *Euchaeta remana* . . . (prosome length of the adult female, ~2.5 mm . . .).